EUROPEAN JOURNAL OF BIOMEDICAL AND PHARMACEUTICAL SCIENCES
http://www.ejbps.com

ISSN 2349-8870
Coden USA: EJBPBO
Volume: 13
Issue: 3
Year: 2026

EUGENOL MITIGATES HIGH-GLUCOSE AND HIGH-LIPID-INDUCED CHANGES IN SKIN FIBROBLASTS

Farzaneh Norouzkhani, Esmaeel Ghasemi Gojani, Bo Wang, DongPing Li, Salma Shujat, Aadarsh Shrestha, Rocio Rodriguez-Juarez, Olga Kovalchuk, Igor Kovalchuk*

Department of Biological Sciences, University of Lethbridge, Lethbridge, AB T1K 3M4.

***Corresponding Author: Igor Kovalchuk**

Department of Biological Sciences, University of Lethbridge, Lethbridge, AB T1K 3M4.

DOI: https://doi.org/10.5281/zenodo.18796572

How to cite this Article: Farzaneh Norouzkhani, Esmaeel Ghasemi Gojani, Bo Wang, DongPing Li, Salma Shujat, Aadarsh Shrestha, Rocio Rodriguez-Juarez, Olga Kovalchuk, Igor Kovalchuk* (2026). Eugenol Mitigates High-Glucose And High-Lipid-Induced Changes In Skin Fibroblasts. European Journal of Biomedical and Pharmaceutical Sciences, 13(3), 201–216.

Article Received on 31/01/2026 **Article Revised on 21/02/2026** **Article Published on 01/03/2026**

ABSTRACT

Eugenol, a phenolic compound derived from clove oil, has garnered considerable attention for its anti-aging properties, particularly in relation to skin health. This study investigated the effects of eugenol on human dermal fibroblasts exposed to high-glucose and high-lipid (HGHL) conditions—25 mM glucose and 400 µM palmitic acid—to mimic premature skin aging. After establishing metabolic stress, fibroblasts were treated with 15 µM eugenol either as a co-treatment or post-treatment. A comprehensive set of assays was conducted, including MTT for cell viability, β-galactosidase staining for senescence, qPCR for inflammatory cytokines and extra-cellular matrix (ECM)-related gene expression, apoptosis and cell cycle analyses, and wound healing assays. Eugenol significantly reduced oxidative stress, inflammation, and cellular senescence in fibroblasts under HGHL conditions. IL-1β and COX-2 expression levels were significantly decreased in both treatment strategies. IL-6 expression was significantly reduced in post-treatment, while TNF-α decreased in co-treatment. Regarding ECM-related genes, COL3A1 expression significantly increased in untreated fibroblasts treated with eugenol, and elastin expression was significantly elevated in co-treatment with HGHL. Additionally, under HGHL conditions, eugenol inhibited apoptosis and positively influenced cell cycle progression, contributing to improved cell survival. Overall, eugenol can be considered as natural compound mitigating signs of metabolic stress-induced skin aging often associated with type II diabetes.

KEYWORDS: cell culture**;** eugenol; skin fibroblasts; skin physiology; anti-aging, inflammation; high-glucose; high-lipid; apoptosis.

INTRODUCTION

Eugenol is a phenolic compound with a chemical formula of $C_{10}H_{12}O_2$, primarily found in clove, cinnamon, and basil. It is biosynthesized through the phenylpropanoid pathway and is contributing to plant defense mechanisms against herbivores and pathogens.[1,2] Beyond its biological role in plants, eugenol has been recognized for its therapeutic potential in dentistry and dermatology, owing to its antimicrobial, anti-inflammatory, antioxidant, and analgesic properties.[3-5] In recent years, it was shown to be relevant to dermatology, addressing skin aging—a complex process driven by both intrinsic factors such as genetic programming and extrinsic factors like UV radiation, pollution, and diet.[6,7]

Skin aging primarily affects the dermis, where extracellular matrix (ECM) degradation, collagen loss, and reduced elasticity contribute to visible signs of aging, including wrinkles, sagging, and skin thinning.[8] These changes are driven by interconnected mechanisms, including oxidative stress, chronic inflammation ('inflammaging'), mitochondrial dysfunction, and DNA damage, all of which exacerbate tissue breakdown and impair repair processes.[9]

Oxidative stress, resulting from an imbalance between reactive oxygen species (ROS) and the skin's antioxidant defenses, is a central contributor to aging. ROS cause damage to proteins, lipids, and DNA, disrupting vital processes such as collagen synthesis and ECM remodeling.[10,11] Additionally, inflammation, particularly

inflammaging, plays a significant role in aging. This process is driven by the upregulation of pro-inflammatory cytokines like TNF-α and IL-6, which activate pathways such as NF-κB and toll-like receptors, contributing to fibroblast senescence and ECM degradation.[12,13]

Mitochondrial dysfunction, another hallmark of aging, leads to decreased ATP production and increased ROS, impairing collagen synthesis and enhancing the cycle of oxidative damage and cellular stress. Dysfunctional mitochondria also activate pro-inflammatory pathways such as AP-1 and NF-κB, further promoting fibroblast senescence and inflammation. The accumulation of senescent fibroblasts in the dermis releases matrix-degrading enzymes, accelerating ECM breakdown and contributing to skin fragility. Additionally, their senescence-associated secretory phenotype amplifies inflammation and ECM degradation, creating a self-reinforcing cycle of aging-related damage.[14,15]

These processes are further amplified in environments characterized by high glucose and high lipid (HGHL) conditions, which exacerbate oxidative stress and promote the formation of advanced glycation end products (AGEs). AGEs form when sugars bind non-enzymatically to proteins, including collagen and elastin, stiffening the ECM and reducing its elasticity. AGEs also trigger inflammatory responses through receptors like RAGE, further accelerating oxidative damage and contributing to skin aging.[16,17]

Eugenol, with its antioxidant, anti-inflammatory, and AGE-reducing properties, presents a promising solution for mitigating skin aging.[18] It has demonstrated potential in treating inflammatory skin conditions like dermatitis and acne while also promoting skin rejuvenation. Advances in nano-encapsulation techniques have further improved eugenol's effectiveness by enhancing its skin penetration and reducing cytotoxicity.[19,20] Despite its potential, the mechanisms underlying eugenol's role in skin aging remain incompletely understood.[21]

While eugenol has numerous benefits for skin aging and therapeutic applications, high concentrations may lead to adverse effects, including liver damage, skin irritation, and DNA damage, underscoring the importance of precise dosage regulation.[22] Its combination of antioxidant, anti-inflammatory, and ECM-preserving properties, along with its light texture and pleasant aroma, makes it a promising ingredient in skincare formulations.[23,24]

This study aims to establish HGHL-induced model of skin aging and to investigate eugenol's antioxidant, anti-inflammatory, and aging-reducing properties in the context of skin aging, particularly in HGHL-induced conditions.

MATERIALS AND METHODS

Chemicals and reagents

The culture medium used was ISCOVE's Modified Dulbecco's Medium (IMDM) 1X (MULTICELL, Cat# 319-106-CL; Wisent Inc., Saint-Jean-Baptiste, QC, Canada). Heat-inactivated Premium Grade Fetal Bovine Serum (Cat# 97068-085, VWR 78 International LLC, Radnor, USA), and 1% Penicillin-Streptomycin (10,000 IU Penicillin and 10 mg/ml Streptomycin, Cat# 450-201-EL, WISENT INC., Quebec, Canada). Additionally, 1X phosphate-buffered saline (PBS) (Cat# 311-010-CL) was obtained from the same supplier. Human foreskin BJ-5ta hTERT-immortalized cell lines (CRL-4001™) were obtained from the American Type Culture Collection (Rockville, MD, USA).

Cell culture and treatments

Human foreskin BJ-5ta hTERT-immortalized cell lines (CRL-4001™), referred to as "fibroblasts" in this study were cultured in ISCOVE's Modified Dulbecco's Medium (IMDM), supplemented with 10% heat-inactivated Premium Grade Fetal Bovine Serum and 1% Penicillin-Streptomycin (10,000 IU Penicillin and 10 mg/ml Streptomycin). All cell culturing and harvesting were conducted in a BSL-2 laboratory. The cells were incubated at 37℃ with 5% CO_2 in a Forma Steri-Cycle CO_2 Incubator (ThermoFisher Scientific, Montreal, Canada) with the culture medium replaced every two days until the cells reached 90%-100% confluency for experimental use. Subculturing was performed weekly. The population doubling (PD) number for each subculture was calculated using the formula $\Delta PD = \log_2(nf/ni)$, where ni represents the initial number of seeded cells and nf the final cell count. Cells between passages 17 and 24 were selected for all experiments.

To induce cell senescence, fibroblasts were exposed to the combination of high-glucose (HG, 25 mM glucose) and high-lipid (HL, 400 µM palmitic acid) (HGHL) conditions for 48 hours. These conditions reduced viability of β-cells, promoted apoptotic behavior, and exacerbated other aging-related effects.[25] A 1.0 M glucose stock solution was prepared by dissolving glucose in the medium, followed by filter sterilization, and stored at 4°C. The palmitic acid (PA) stock solution was prepared by dissolving PA in 100% ethanol with heating at 70°C. The dissolved PA was then combined with sterile 10% BSA and underwent two cycles of heating at 55°C for 15 minutes with mixing. The PA stock was aliquoted and stored at −20°C. Prior to use, the PA stock was reheated at 55°C for 15 minutes.

Based on various studies, pilot experiments, and repeated tests assessing cell toxicity and viability, we optimized the application of eugenol (CAS No. 97-53-0, Sigma-Aldrich, Saint Louis, MO, USA) for co-treatment and post-treatment conditions, selecting concentrations of 15 µM for both experimental settings.

For post-treatment approach, fibroblasts were exposed to HGHL conditions for 48 hours to induce senescence. Following this, the HGHL-treated wells were washed twice with 1X PBS and treated either with 15 µM eugenol or medium alone for an additional 48 hours. The experimental setup included two additional wells that were not exposed to HGHL. One served as the untreated control containing only medium (CT), while the other was treated with 15 µM eugenol (E15) to evaluate its effect on untreated fibroblasts. These conditions allowed comparisons between medium-only and eugenol treatments on HGHL-induced fibroblasts and their respective non-HGHL counterparts.

The co-treatment approach investigated eugenol's protective effects during simultaneous exposure to HGHL. Fibroblasts were treated with 15 µM eugenol alongside HGHL for 48 hours. The experimental design consisted of four wells: one containing untreated fibroblasts with medium only (CT), one treated with HGHL alone (control for HGHL-induced damage), one treated with 15 µM eugenol alone (E15) on untreated fibroblasts, and one with the combined treatment of HGHL and 15 µM eugenol. This setup enabled the evaluation of eugenol's protective capabilities under HGHL conditions.

These concentrations were selected for all assays, including wound healing, beta-galactosidase, apoptosis, and cell cycle analyses, along with RNA isolation for qPCR.

MTT assay

Metabolic activity, as a reflection of cell viability in BJ-5ta human skin fibroblasts was measured using the MTT assay (3-[4,5-dimethylthiazol-2-yl]-2,5-diphenyltetrazolium bromide; thiazolyl blue) with the Cell Proliferation Kit I (#11465007001, Roche, Ontario, Canada) as per the manufacturer's instructions. Fibroblasts were seeded at 5.0 x 10^3 cells/well in 100 µL of culture medium in 96-well plates and incubated for 24-48 hours based on confluency before treatment. A range of treatments, including HGHL and eugenol, were tested to determine cytotoxic or effective doses. All measurements were done in triplicate at intervals of 0, 1, 2, and 3 days. After treatment, 10 µL of MTT reagent was added directly to each well and incubated for 4 hours at 37°C in a humidified environment with 5-6.5% CO_2, followed by 100 µL of MTT solubilization solution (10% SDS in 0.01 M HCl) and overnight incubation at 37°C with 5-6.5% CO_2. Finally, absorbance was read at 595 nm using a plate reader (FLUOstar Omega, BMG LABTECH, Offenburg, Germany). Cell viability was calculated relative to controls. Experiments were repeated three times with triplicates in each test.

β-galactosidase assay

To assess cellular senescence, fibroblasts were treated under various conditions, including HGHL to induce premature aging, eugenol co-treatment and post-treatment, as well as eugenol treatment on untreated fibroblasts. The cells were then washed twice with 1x PBS. To quantify β-galactosidase activity, fibroblast lysates from both normal and HGHL-induced prematurely aged fibroblasts were prepared using the protein lysis buffer from the Beta-Galactosidase Detection Kit (Fluorometric) (ab176721, Abcam, Toronto, ON, Canada). Protein concentration in each sample was measured with the Bradford assay, and the samples were diluted to a final protein concentration of 1 µg/ml. Following this, 50 µl of each standard and sample (diluted in 1× lysis buffer) were transferred to a black 96-well plate. To each well, 50 µl of fluorogenic fluorescein digalactoside (FDG) working solution was added, and the plate was incubated at 37°C for 4 hours. Subsequently, 50 µl of stop buffer was added, and fluorescence was measured for each sample using a FLUOstar Omega (BMG LABTECH, Offenburg, Germany) plate reader with excitation and emission wavelengths of 490 nm and 525 nm, respectively. β-galactosidase levels, indicating cellular senescence, were determined by comparing fluorescence values to a β-galactosidase standard curve prepared for each experiment. Experiments were repeated three times with triplicates in each test.

qRT-PCR

RNA was extracted from fibroblast monolayer cultures using TRIzol® Reagent (Invitrogen, Carlsbad, CA), followed by purification with the RNeasy kit (Qiagen, Toronto, ON, Canada) as per the manufacturer's protocol. RNA concentration was measured using a NanoDrop 2000c spectrophotometer (ThermoFisher Scientific, Wilmington, DE). A fraction of the total RNA was employed to synthesize complementary DNA (cDNA), utilizing 1 µg of total RNA and a specialized cDNA synthesis kit known as iScript™ Reverse Transcription Supermix (Cat: 1708841; BioRad Laboratories, Saint-Laurent, QC, Canada). The resulting cDNA product was then employed as a template for q-PCR, with 1 µl of cDNA being utilized in each reaction. The qRT-PCR reactions were carried out using a SsAdvancedTM Universal Inhibitor-Tolerant SYBR Green Supermix (Cat: 1725017; BioRad Laboratories, Saint-Laurent, QC, Canada). The primers required for the q-RT-PCR analysis were designed employing an online IDT software (Table 1). Beta-actin was used as the reference gene for normalization in the experiment. Each group included three biological replicates, with three technical replicates per sample.

Table 1: Primers used in the experiment.

Gene	Primer sequence
Col3a1	
H-F-Col3a1	F: 5' AAGTCAAGGAGAAAGTGGTCG 3'
H-R-Col3a1	R: 5' CTCGTTCTCCATTCTTACCAGG 3'
Col1a1	
H-F-Col1a1	F: 5' CCCCTGGAAAGAATGGAGATG 3'
H-R-Col1a1	R: 5' TCCAAACCACTGAAACCTCTG 3'
Elastin	
H-F-Eln	F: 5' GGCTTTGGTGTCGGAGTC 3'
H-R-Eln	R: 5' AACTAACCCGTACTTGGCAG 3'
β-Actin	
Forward	F: 5' GGCATCCTCACCCTGAAGTA 3'
Reverse	R: 5' CACACGCAGCTCATTGTAGAAG 3'
IL-6	
Forward	F: 5' GGAGACTTGCCTGGTGAAA 3'
Reverse	R: 5' CTGGCTTGTTCCTCACTACTC 3'
COX-2	
Forward	F: 5' TACTGGAAGCCAAGCACTTT 3'
Revers	R: 5' GGACAGCCCTTCACGTTATT 3'
TNF-alpha	
Forward	F: 5' CCAGGGACCTCTCTCTAATCA 3'
Reverse	R: 5' TCAGCTTGAGGGTTTGCTAC 3'
IL-1β	
Forward	F: 5' CCTTAGGGTAGTGCTAAGAGGA 3'
Reverse	R: 5' AAGTGAGTAGGAGAGGTGAGAG 3'

Wound healing assay

Fibroblasts were grown in 6-well plates until they reached over 90% confluence. A 100 µL pipette tip was employed to create a scratch or wound line down the center of each well, mimicking a wound scenario. Following this, the fibroblasts were washed twice with 1X PBS before adding the appropriate cell culture growth medium or specific treatments. Images of the wound healing process were captured at various time points: day 0 (2 hours after wound creation, treatments began at this time), day 1 (24 hours after treatment), day 2 (48 hours after treatment), day 3 (72 hours after treatment) and day 4 (96 hours after treatment). The Infinity3 camera with OLYMPUS CKX41 microscope was utilized to obtain images within its linear dynamic range, which ensures a consistent relationship between signal intensity and the amount of material present. The migration distance of fibroblasts (µm), indicating their wound-closing ability, was measured throughout the experiment. Image analysis was conducted using ImageJ (IJ 1.46r) software, and all samples were analyzed in triplicate.

Cell cycle assay

After inducing fibroblast treatments, the fibroblasts were washed twice with cold 1X PBS to remove residual medium and non-adherent fibroblasts. Next, they were trypsinized to detach them from the culture surface and then centrifuged to collect the cell pellet. The pellet was resuspended in cold 1X PBS and fixed by adding cold 70% ethanol dropwise while gently vortexing. The fibroblasts were then incubated at 4℃ for at least 2 hours (or overnight) to ensure proper fixation.

Following fixation, the fibroblasts were washed again with cold PBS to remove ethanol. To eliminate RNA, 50 µL of RNase solution (100 µg/mL) was added to each sample, followed by the addition of 200 µL of a propidium iodide (PI) solution prepared at 50 µg/mL to stain the DNA. The stained cells were incubated in the dark at room temperature for 30-60 minutes to ensure consistent dye binding.

Finally, the cell cycle distribution was analyzed by BD FACSAria™ Fusion Flow Cytometer (BD Biosciences, San Diego, CA, USA). Fibroblasts were categorized based on DNA content into different phases: G0/G1 (resting or initial growth phase), S (DNA synthesis phase), and G2/M (second growth and mitosis phase), providing insights into the cell population's distribution across the cell cycle stages.

Apoptosis assay

After treating fibroblasts and washing them twice with 1X PBS to remove any residual medium and non-adherent fibroblasts, the fibroblasts were trypsinized to detach them from the culture plate. They were then centrifuged to collect the cell pellet, which was resuspended in cold PBS. To detect apoptosis, the fibroblasts were stained with Annexin V-FITC and PI, which allows to distinguish between live, early apoptotic, late apoptotic, and necrotic cells.

Annexin V binds to phosphatidylserine, which translocates to the outer layer of the cell membrane early in apoptosis. PI, a DNA-binding dye, only enters fibroblasts with compromised membranes, marking late apoptotic and necrotic cells. The staining solution containing Annexin V-FITC and PI was gently mixed with the cell suspension and incubated in the dark at room temperature for 15-20 minutes.

The stained fibroblasts were then analyzed using flow cytometry (BD FACSAria™ Fusion Flow Cytometer, BD Biosciences, San Diego, CA, USA). Fibroblasts that were Annexin V-positive and PI-negative were classified as early apoptotic, while fibroblasts that were both Annexin V- and PI-positive were considered late apoptotic or necrotic. This assay allowed quantification of the apoptotic and necrotic cell populations, providing insights into the treatment's effects on cell viability and apoptosis.

Statistics

The collected data was subjected to statistical analysis using one-way analysis of variance (ANOVA), followed by Dunnett's test for comparing mean values. GraphPad Prism 6 software was used to perform the analysis and prepare the graphics.

RESULTS

Eugenol increases cellular viability in the untreated and HGHL-treated samples

A pilot study was conducted to assess cell viability across eugenol concentrations ranging from 5 to 20 µM. The findings revealed that concentrations between 5 and 15 µM enhanced cell viability, measured by the analysis of metabolic activity, whereas 20 µM decreased it (Supplementary figure 1). Thus, for the co- and post-treatment experiments, we limited the eugenol dose to 15 µM.

Analysis showed that exposure of untreated fibroblasts to E15 resulted in significant increase in cell viability in both post-treatment and co-treatment experiments (Figure 1). In the post-treatment experiment, E15 showed the highest cell viability under conditions altered by HGHL (Figure 1A). Similarly, in the co-treatment experiment, E15 was also the most effective (Figure 1B). In both cases, we observed dose-dependent increase in cell viability when eugenol was applied to HGHL-treated cells. Therefore, E15 was selected for all subsequent experiments.

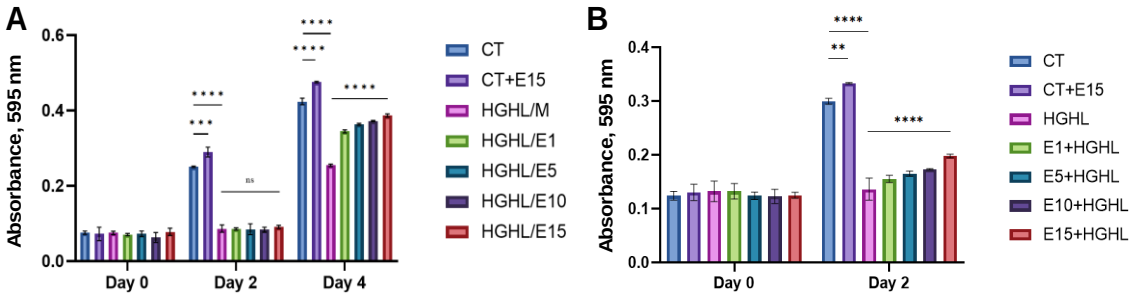

Figure 1: Effects of different concentrations of eugenol on the cell viability in post-treatment (A) and co-treatment (B) of HGHL-induced fibroblasts. Data shows the cell viability (MTT assay). Y axis shows absorbance at 595 nm in fibroblasts measured at days 0, 2 and 4 after eugenol application in HGHL post-treatment (A) and day 0 and day 2 of co-treatment of eugenol and HGHL (B). CT - Control (untreated fibroblasts); CT+E15 - eugenol 15 µM added to untreated fibroblasts; E1, E5, E10, E15 - eugenol at 1, 5, 10, 15 µM; HGHL - high glucose (25 mM) and high lipid (400 µM) treatment; HGHL/M – medium added to HGHL treatment sample; HGHL/E1, E5, E10, E15 - eugenol at various doses added post HGHL induction; E1, E5, E10, E15+HGHL- eugenol at different doses added together with HGHL as a co-treatment. Data are presented as mean ± SD, N=3. The collected data was subjected to statistical analysis using one-way analysis of variance (ANOVA), followed by Dunnett's test for comparing mean values. GraphPad Prism 6 software was used to perform this analysis. The asterisks show significant difference, three - p<0.001; four - p<0.0001; ns – non-significant.

Eugenol causes a reduction in beta-galactosidase activity in the untreated and HGHL-treated fibroblasts

Beta-galactosidase levels, a marker of cellular senescence, increase with aging. Analysis showed the highest beta-galactosidase activity in a HGHL-treated sample in co-treatment (Figure 2B), and in a HGHL-treated sample followed by addition of culture medium in post-treatment (HGHL/M, Figure 2A). Beta-galactosidase activity of other samples was significantly lower than HGHL-treated samples in both co- and post-treatments. This experiment showed that eugenol can prevent the increase in cellular senescence in response to HGHL in co-treatment experiment (Figure 2B) as well as decreases the cellular senescence caused by HGHL in post-treatment experiment (Figure 2A).

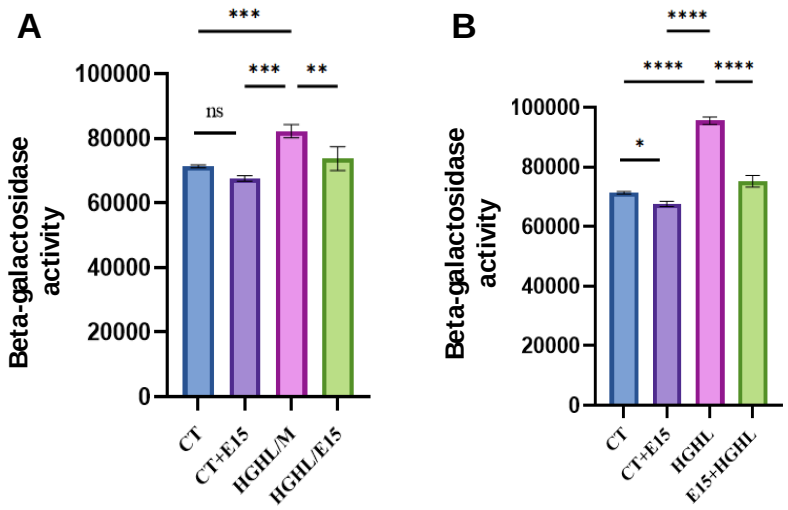

Figure 2: Effects of eugenol on beta-galactosidase activity in fibroblasts treated with HGHL. Data shows the beta-galactosidase activity (measured in fluorescence intensity, arbitrary units, Y axis) after HGHL treatment in post- (A) and co-treatment experiments (B) with eugenol. CT - Control (untreated fibroblasts); CT+E15 - eugenol 15 µM added to untreated fibroblasts; HGHL - high glucose (25 mM) and high lipid (400 µM) treatment; HGHL/M – medium added to HGHL treatment sample; HGHL/E15 - 15 µM eugenol added post HGHL induction; E15+HGHL - 15 µM eugenol added together with HGHL as a co-treatment. Data are presented as mean ± SD. N=3. Statistical analysis was performed using one-way ANOVA, followed by Dunnett's test for mean comparisons, with GraphPad Prism 6 software. Significance indicators: ***p < 0.001, ****p < 0.0001; ns - non-significant.

Eugenol reduces apoptosis in the HGHL-treated fibroblasts

For both co- and post-treatment with eugenol, the results showed that HGHL and HGHL followed by medium (HGHL/M) significantly induced apoptosis compared to CT (Figure 3). Exposure of untreated fibroblasts to E15 resulted in a nonsignificant increase in apoptosis (Figure 3A, B). Both E15 treatments significantly reduced apoptosis (Figure 3A and B).

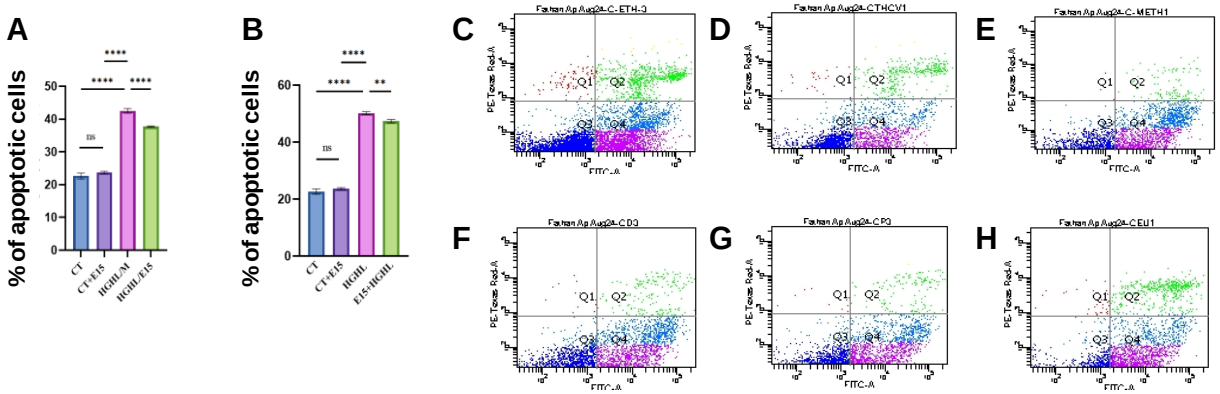

Figure 3: Effects of eugenol on apoptosis in the untreated and HGHL-treated fibroblasts. Data shows the percentage of apoptotic cells after HGHL treatment in post- (A) and co-treatment (B) experiments with eugenol. Representative images of apoptosis in Ct (C), Ct+E15 (D), HGHL (E), HGHL/M (F), HGHL/E15 (G), E15+HGHL (H). CT - control (untreated fibroblasts); CT+E15 - eugenol 15 µM added to untreated fibroblasts; HGHL - high glucose (25 mM) and high lipid (400 µM) treatment; HGHL/M – medium added to HGHL treatment sample; HGHL/E15 - 15 µM eugenol added post HGHL induction; E15+HGHL - 15 µM eugenol added together with HGHL as a co-treatment. Data are presented as mean ± SD. N=3. Statistical analysis was performed using one-way ANOVA, followed by Dunnett's test for mean comparisons, with GraphPad Prism 6 software. Significance indicators: ***p < 0.001, ****p < 0.0001; ns - non-significant.

Eugenol alleviates stress and enhances the cell cycle in the HGHL-induced fibroblasts

In the cell cycle assay, fibroblasts were categorized into distinct phases based on DNA content: G0/G1 (resting or initial growth phase), S (DNA synthesis phase), and G2/M (second growth and mitosis phase), allowing for an analysis of the fibroblast population's distribution across these stages. Both co-treatment and post-treatment

with HGHL and HGHL/M induced significant cellular stress, leading to a shift of many fibroblasts into the S/G2 phases and disrupting normal cell cycle progression (Figure 4).

When treated with E15 alone, there was a notable increase and alteration in the cell cycle compared to control conditions (Figure 4A, B). However, post-treatment with eugenol significantly alleviated the stress caused by the HGHL environment, preserving a higher proportion of fibroblasts in the G1 phase and reducing the number of cells in the S/G2 phases (Figure 4A).

Similarly, co-treatment with eugenol significantly mitigated the stress induced by the HGHL environment (Figure 4B). Eugenol demonstrated protective and restorative effects on the cell cycle under HGHL conditions, highlighting its potential to counteract stress-induced disruptions in cellular function.

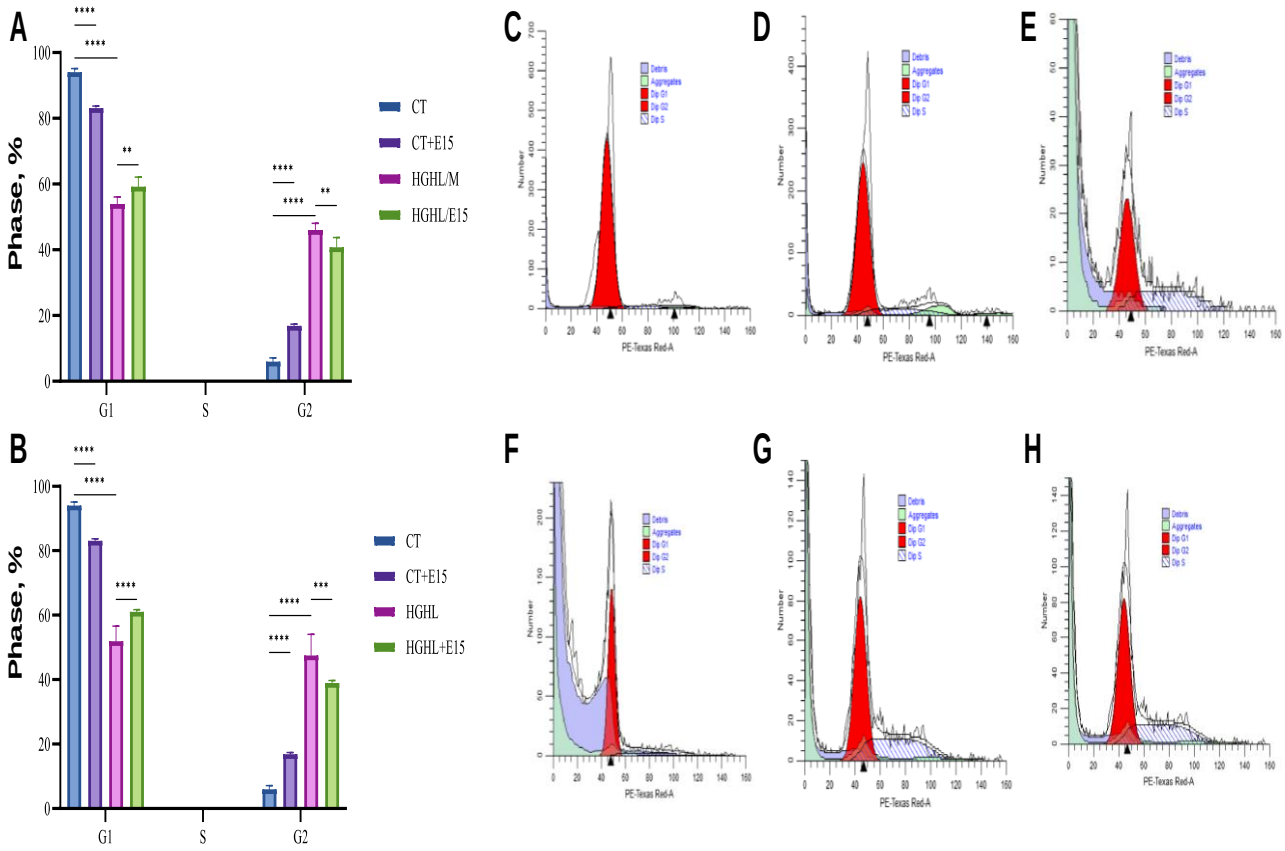

Figure 4: Impact of eugenol on the cell cycle in the untreated and HGHL-treated fibroblasts. Data shows the percentage of cells in specific cell cycle phase after HGHL treatment in post- (A) and co-treatment (B) experiments with eugenol. Representative images of cell cycle in Ct (C), Ct+E15 (D), HGHL (E), HGHL/M (F), HGHL/E15 (G), E15+HGHL (H). CT - control (untreated fibroblasts); CT+E15 – eugenol 15 µM added to untreated fibroblasts; HGHL - high glucose (25 mM) and high lipid (400 µM) treatment; HGHL/M – medium added to HGHL treatment sample; HGHL/E15 - 15 µM eugenol added post HGHL induction; E15+HGHL - 15 µM eugenol added together with HGHL as a co-treatment. Data are presented as mean ± SD. N=3. Statistical analysis was conducted using one-way ANOVA, followed by Dunnett's test for mean comparisons, using GraphPad Prism 6 software. Significance indicators: ***p < 0.001, ****p < 0.0001; ns - not significant.

Eugenol does not significantly improve wound healing in the untreated and HGHL-treated fibroblasts

The wound healing assay is commonly used to assess the anti-aging effects of various compounds by evaluating fibroblast proliferation and migration. E15 applied to untreated fibroblasts did not significantly change the wound healing (Figure 5). Exposure to HGHL significantly impaired wound healing compared to the control group and adding medium (HGHL/M group) did not lead to any improvement (Figure 5). Co-treatment and post-treatment with E15 and HGHL did not improve the wound healing.

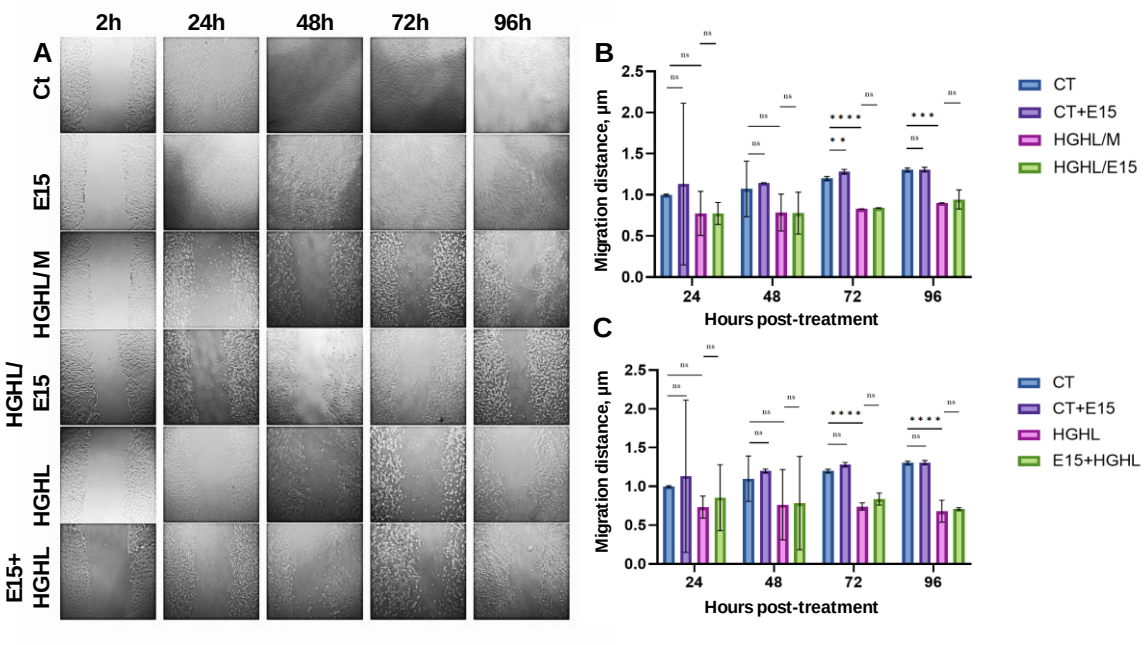

Figure 5: Effects of eugenol on wound healing progress in the untreated and HGHL-treated fibroblasts. A. Microscope images depict the wound healing process in untreated and HGHL-treated fibroblasts under various treatment conditions. For post-treatments, HGHL was applied 2 hours after wound creation and continued for 48 hours. After 48 hours, HGHL was removed, fibroblasts were washed with 1X PBS, and treatments with E15 and medium were applied for an additional 48 hours (HGHL/E15). Additional conditions included: untreated fibroblasts treated with E15 (Ct+E15), where E15 was added 2 hours after wound creation; fibroblasts co-treated with HGHL and E15 simultaneously 2 hours post-wound creation (E15+HGHL); fibroblasts treated with HGHL alone 2 hours after wound creation (HGHL), and CT. Images were taken at specific intervals: 2 hours post-wound creation, and at 24-, 48-, 72- and 96-hours following treatment. Wound closure was quantified using ImageJ software. The 2-hour images for each well were intended to be consistent; however, manual processing with 100-µL pipette tips introduced variability. Thus, images at subsequent time points were normalized using their respective 2-hour images as references. B. Quantitative analysis of wound healing progression in HGHL-induced fibroblasts post-treated with E15. C. Quantitative analysis of wound healing progression in fibroblasts co-treated with HGHL and E15. Data are shown as mean ± SD. N=3. Statistical significance was determined using one-way ANOVA, followed by Dunnett's post hoc test in GraphPad Prism 6 software. Significance levels: ***p < 0.001, ****p < 0.0001; ns - not significant.

Protective effects of eugenol on the expression of genes involved in the extracellular matrix maintenance and inflammatory response in untreated and HGHL-treated fibroblasts

Fibroblasts are key producers of essential ECM components—such as collagen, elastin, and hyaluronan—that are critical for maintaining the structure and function of the skin as well as other tissues and organs throughout the body. Additionally, inflammatory cytokines play a crucial role in skin health, as they regulate collagen synthesis and influence the skin's ability to repair and renew, highlighting the importance of assessing these factors in studies of cellular aging and tissue resilience.

Here, we first tested the expression of two collagen encoding genes, *Collagen type I alpha 1* (*COL1A1*), *Collagen type III alpha 3* (*COL3A1*), and *elastin* (*ELN*) gene.

Exposure to E15 in untreated fibroblasts significantly reduced the expression of *COL1A1* and *ELN* genes (Figures 6A, 6B, 6E, 6F), while it significantly increased the expression of *COL3A1* (Figures 6C, 6D). HGHL treatment led to a decrease in the expression of all three genes, both in co-treatment and post-treatment scenarios. When E15 was added during post-treatment, it had no significant effect on *COL1A1* and *COL3A1* expression levels, but it further downregulated *ELN* expression (Figures 6A, 6C, 6E). In contrast, co-treatment of E15 with HGHL did not change *COL1A1* and *COL3A1* expression. However, it did result in a significant increase in *ELN* expression (Figures 6B, 6D, 6F).

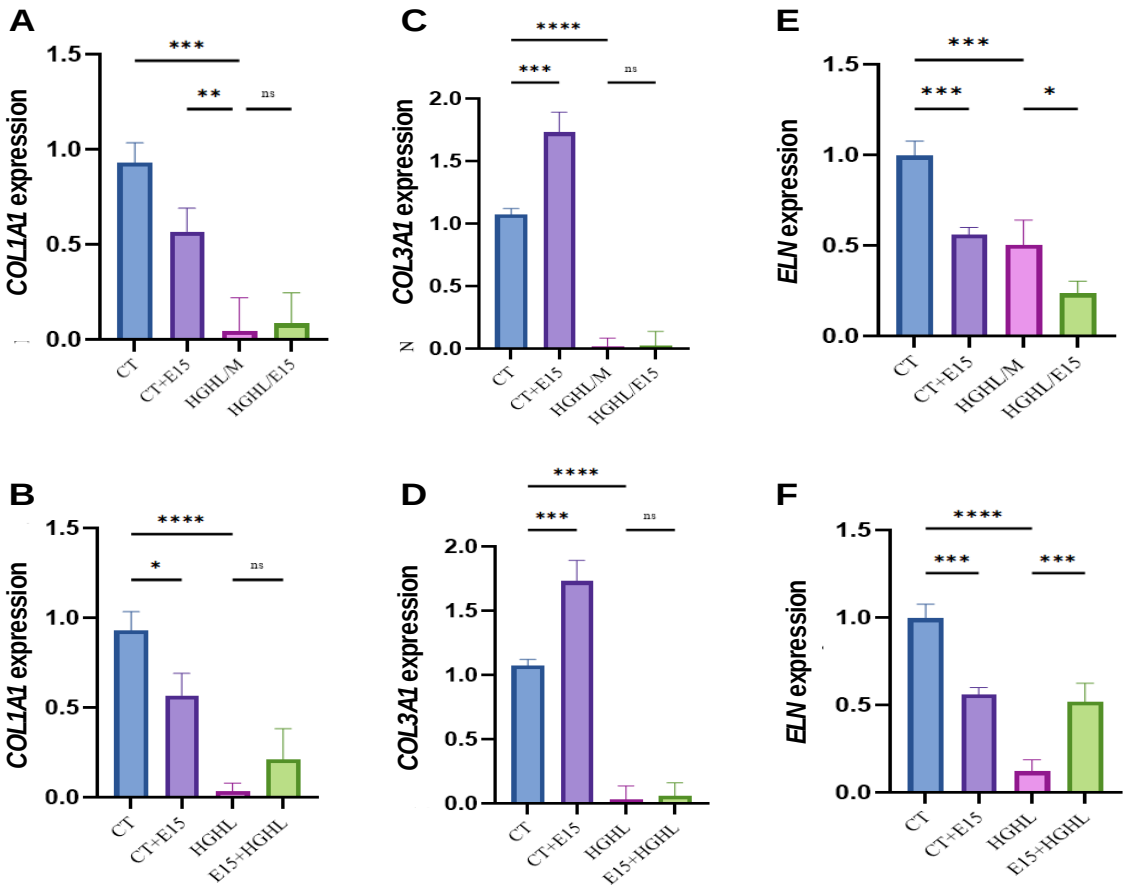

Figure 6: Effect of eugenol on the expression of *COL1A1*, *COL3A1* and *ELN* genes in the untreated and HGHL-treated fibroblasts. COL1A1 expression in post-treatment (A) and co-treatment (B). COL3A1 expression in post-treatment (C) and co-treatment (D). ELN expression in post-treatment (E) and co-treatment (F). CT - control (untreated fibroblasts); CT+E15 – eugenol 15 µM added to untreated fibroblasts; HGHL - high glucose (25 mM) and high lipid (400 µM) treatment; HGHL/M – medium added to HGHL treatment sample; HGHL/E15 - 15 µM eugenol added post HGHL induction; E15+HGHL - 15 µM eugenol added together with HGHL as a co-treatment. Data are presented as mean ± SD. N=3. Statistical analysis was performed using one-way ANOVA, followed by Dunnett's test for mean comparisons, using GraphPad Prism 6 software. Significance indicators: ***p < 0.001, ****p < 0.0001; ns - not significant.

In the analysis of inflammatory cytokine gene expression, the addition of E15 to untreated fibroblasts significantly decreased the expression of *IL-1β, IL-6*, and *COX-2* genes, with a non-significant decrease in *TNF-α* expression (Figure 7). HGHL treatment, on the other hand, significantly increased the expression of all tested genes in both co-treatment and post-treatment experiments. In the post-treatment experiment, the addition of E15 after HGHL treatment significantly reduced the expression of all genes, except for *TNF-α* (Figures 7A, 7C, 7E, 7G). In the co-treatment experiment, E15 significantly reduced the expression of all genes, except *IL-6*, which was increased, when compared to HGHL treatment alone (Figures 7B, 7D, 7F, 7H).

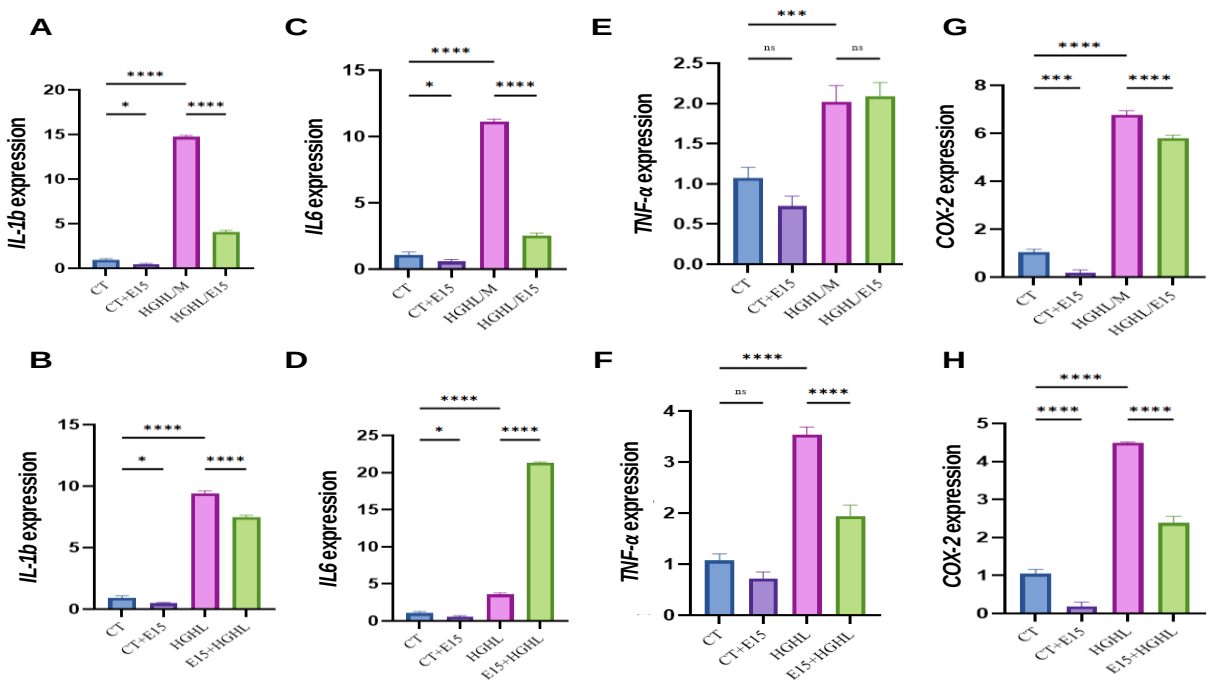

Figure 7: Effect of eugenol on the expression of inflammatory cytokines in the untreated and HGHL-treated fibroblasts. *IL-1β* expression in post-treatment (A) and co-treatment (B). *IL-6* expression in post-treatment (C) and co-treatment (D). *TNF-α* expression in post-treatment (E) and co-treatment (F). *COX-2* expression in post-treatment (G) and co-treatment (H). CT - control (untreated fibroblasts); CT+E15 – eugenol 15 µM added to untreated fibroblasts; HGHL - high glucose (25 mM) and high lipid (400 µM) treatment; HGHL/M – medium added to HGHL treatment sample; HGHL/E15 - 15 µM eugenol added post HGHL induction; E15+HGHL - 15 µM eugenol added together with HGHL as a co-treatment. Data are presented as mean ± SD. N=3. Statistical analysis was performed using one-way ANOVA, followed by Dunnett's test for mean comparisons, using GraphPad Prism 6 software. Significance indicators: ***p < 0.001, ****p < 0.0001; ns - not significant.

Supplementary Materials

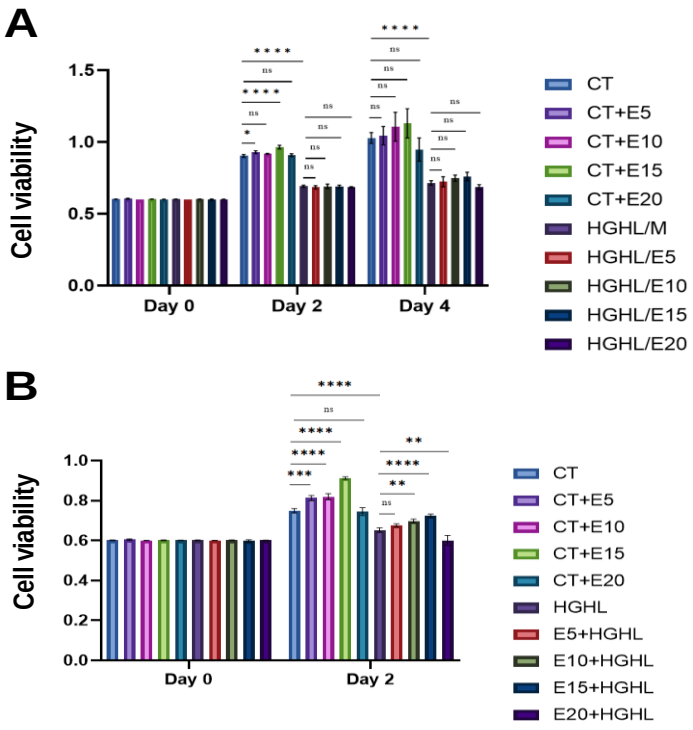

Supplementary Figure 1. Effects of Different Concentrations of Eugenol on the Cell Viability in Post-treatment (A) and Co-treatment (B) of Untreated and HGHL-Induced fibroblasts. Data shows the cell viability (MTT

assay) Y axis shows absorbance at 595 nm) of fibroblasts measured at days 0, 2 and 4 after HGHL treatment (A) and day 0 and day 2 co-treatment of eugenol and HGHL (B). CT - Control (untreated fibroblasts); CT+E5, E10, E15 and E20 - eugenol 5, 10, 15 and 20 µM added to untreated fibroblasts; E5, E10, E15, E20 - eugenol at 5, 10, 15, 20 µM; HGHL - high glucose (25 mM) and high lipid (400 µM) treatment; HGHL/M – medium added to HGHL treatment sample; HGHL/E5, E10, E15, E20 - eugenol at various doses added post HGHL induction; E5, E10, E15, E20+HGHL- eugenol at different doses added together with HGHL as a co-treatment. Data are presented as mean ± SD. N=3. The collected data was subjected to statistical analysis using one-way analysis of variance (ANOVA): followed by Dunnett's test for comparing mean values. GraphPad Prism 6 software was used to perform this analysis. The asterisks show significant difference, three - p<0.001; four - p<0.0001; ns – non-significant.

DISCUSSION

In this study, we developed an in vitro model of skin aging by exposing fibroblasts to a combination of high glucose (25 mM) and high lipid (palmitic acid 400 µM) conditions. This approach was designed to mimic an environment associated with metabolic stress, commonly observed in conditions like obesity and type 2 diabetes. In this study, we showed that the combination of these two metabolic stressors not only induced cellular senescence but also resulted in alterations in cell viability, cell cycle progression, and apoptosis. Additionally, we observed significant changes in the expression of inflammatory and ECM-related genes encoding collagen and elastin. Furthermore, wound healing assays demonstrated a decline in fibroblast migration under HGHL conditions.

Research has consistently shown that high glucose levels can accelerate the aging process in various cell types, including fibroblasts, through mechanisms such as increased oxidative stress, the formation of AGEs, and the activation of senescence pathways. For example, studies by Bian et al. (2020)[26] and Chang et al. (2010)[27] demonstrated that chronic exposure to elevated glucose levels induced senescence in human dermal fibroblasts and endothelial cells, respectively, primarily through the accumulation of AGEs and subsequent activation of inflammatory pathways. Exposure to high glucose levels significantly reduced cell viability across various cell types, including fibroblasts. For instance, Zhang et al. (2019) showed that exposure to high glucose (50 mM) in retinal pigment epithelial (RPE) cells led to increased ROS generation, apoptosis, and reduced proliferation and mitophagy.[28]

Similarly, high lipid conditions have been implicated in promoting cellular stress and senescence. High lipid condition is commonly associated with metabolic diseases, and its effects on cellular aging have been explored in several studies. For instance, studies by Romer et al. (2021)[29] and Oberhauser et al. (2021)[30] showed that high lipid-induced lipotoxicity in various cell types, including adipocytes, hepatocytes and beta-cells, led to cellular inflammation, mitochondrial dysfunction, and premature senescence.

The effect of HGHL was demonstrated on beta cells; Gojani et al. (2023) reported that exposure to high glucose (25 mM) and palmitic acid (400 µM) for 48 hours in beta cells decreased viability and induced apoptosis, highlighting the compounded effects of metabolic stressors.[25] However, prior to our investigation, the combined effect of HGHL conditions on dermal fibroblasts had not been studied. Additionally, most studies have primarily focused on UV radiation or H_2O_2-induced aging in skin fibroblasts, while metabolic aging has received less attention, despite its growing relevance.[31,32]

Effect of HGHL and eugenol on cell viability and senescence

Previous research showed that eugenol promotes cell viability. Absalan et al. (2017) demonstrated that eugenol improved viability and reduced aging markers in human adipose-derived stem cells.[33]

In our study, the 15 µM eugenol treatment (E15) significantly enhanced fibroblast viability under both normal and HGHL conditions. E15 showed no cytotoxicity in untreated cells and, notably, produced the highest viability compared to the control group and other eugenol concentrations tested. Moreover, E15 was the most effective dose when used as a post-treatment or co-treatment with HGHL, outperforming HGHL alone, HGHL/M, and other eugenol concentrations.

The reduction in the cell viability in response to HGHL is not only indicative of cytotoxicity but may suggest a progression toward cellular senescence, a central feature of aging. Increased activity of senescence-associated β-galactosidase (SA-β-gal) is a widely recognized marker of senescence.[34] Preclinical studies have shown that senescent cells are a major source of proinflammatory factors in the adipose tissue of obese mice. Although the relationship between adipose senescence and obesity-related complications in humans is less clear, emerging evidence highlights the role of metabolic stress in promoting senescence. For instance, Rouault et al. (2021) demonstrated that high glucose exposure increases SA-β-gal activity, further linking metabolic stress to the onset of cellular aging and metabolic disease.[35] Consistent with these findings, our results revealed a significant increase in SA-β-gal activity in fibroblasts under HGHL conditions, confirming the induction of cellular senescence.

Building on this, we examined the effects of eugenol on cellular senescence. As expected, HGHL exposure

elevated β-gal activity, indicating enhanced senescence. However, treatment with 15 μM eugenol reduced β-galactosidase activity in untreated fibroblasts compared to all other groups, including the control, suggesting a potential anti-senescence effect even under basal conditions. Notably, both co-treatment and post-treatment with E15 effectively significantly lowered β-gal activity compared to HGHL and HGHL/M treatments, demonstrating eugenol's ability to attenuate senescence even under metabolic stress. These findings support the hypothesis that eugenol mitigates the accumulation of senescent cells, contributing to its protective role in skin aging.[7]

Effect of HGHL and eugenol on cell cycle

In addition to promoting senescence, HGHL conditions have also been associated with dysregulated cell cycle progression. Our findings align with previous studies highlighting the impact of metabolic stress on cell cycle regulation. Kim et al. (2019) demonstrated that high glucose and insulin levels promote cell cycle progression in bladder epithelial cells by upregulating cyclins (e.g., cyclin D) and cyclin-dependent kinases (Cdk4, Cdk2), facilitating S phase entry.[33] Similarly, Xu et al. (2023) reported that elevated lipid levels activate lipid biosynthesis through squalene epoxidase (SQLE), promoting proliferation and advancing cell cycle progression.[36]

Because of HGHL stress, cells experience oxidative damage, which activates DNA damage checkpoints during the S and G2 phases to pause the cycle and allow for repair. The accumulation of cells in these phases reflects an adaptive response aimed at preventing the propagation of damaged DNA, making S/G2 arrest a well-known hallmark of cellular stress.[37] In line with this, our cell cycle analysis showed a significant increase in the proportion of fibroblasts in the G2 phase following HGHL exposure, indicating disrupted regulatory control and elevated cellular stress.

Eugenol, on the other hand, has been shown to arrest cell cycle progression in the S phase and inhibit E2F1 activity in melanoma cells, resulting in growth suppression.[38] In our study, E15 treatment maintained normal cell cycle progression under control conditions by retaining a higher proportion of cells in the G1 phase. Moreover, E15 effectively countered the cell cycle disruption caused by HGHL, reducing the percentage of cells in the S/G2 phase and restoring cell cycle balance. These results suggest that eugenol supports cellular homeostasis and fibroblast function by modulating the cell cycle under both normal and stress-induced conditions.

3.3 Effect of HGHL and eugenol on apoptosis

Cell cycle progression and apoptosis are distinct processes, but disturbances in either can lead to significant effects on cellular function and survival. Apoptosis assays revealed that HGHL conditions induce apoptosis compared to other treatments, which aligns with previous studies. For instance, research on the role of TSPAN8 in regulating autophagy and apoptosis in HK-2 cells exposed to high glucose conditions demonstrated that high glucose could trigger apoptosis in various cell types, mimicking the environment of diabetic nephropathy.[39] Additionally, another study showed that HGHL conditions induce significant apoptosis in pancreatic β-cells, impairing insulin secretion.[13] Treatment with telmisartan effectively reduced this HGHL-induced apoptosis, further emphasizing the detrimental impact of HGHL levels on β-cell function.[13]

Eugenol has also been shown to offer protective effect against transmissible gastroenteritis virus (TGEV)-induced intestinal damage. It achieves this by reducing oxidative stress and inhibiting apoptosis in intestinal epithelial cells. Studies have demonstrated that eugenol supplementation lowers ROS levels, thereby decreasing oxidative stress and preventing apoptosis in both *in vitro* and *in vivo* models of TGEV infection.[40]

In our study, HGHL conditions induced significant apoptosis in fibroblasts, reflecting the detrimental effects of these stressors. Eugenol significantly reduced apoptosis induced by HGHL, suggesting that eugenol can protect against stress-induced cell death. These findings align with existing research demonstrating eugenol's potential in modulating apoptosis, particularly under stress conditions.[40]

Effect of HGHL and eugenol on the expression of proinflammatory cytokines

Elevated glucose and lipid levels are known to impair wound healing by increasing the expression of proinflammatory cytokines, reducing collagen and elastin gene expression, and disrupting cell migration. These metabolic imbalances activate intracellular signaling pathways that trigger inflammatory responses.[41] In fibroblasts, high glucose conditions have been shown to upregulate cytokines such as *IL-6* and *TNF-α*, primarily through activation of the nuclear factor kappa B (NF-κB) pathway, as demonstrated by Du et al. (2016).[42] and Shi et al. (2019).[43] Similarly, Hasan et al. (2019) reported that palmitate, a saturated fatty acid, stimulates *IL-6* and *TNF-α* expression in fibroblasts via the Toll-like receptor 4 (TLR4) signaling pathway.[44]

In our study, HGHL conditions led to a marked increase in inflammatory cytokine expression in dermal fibroblasts, consistent with previous findings. Our findings showed that both post-treatment and co-treatment with eugenol significantly reduced *IL-1β* and *COX-2* expression compared to HGHL/M and HGHL alone, highlighting eugenol's consistent anti-inflammatory effect.

In the case of *IL-6*, the highest expression was observed in fibroblasts treated with HGHL/M. Post-treatment with

E15 led to a significant reduction in *IL-6* levels, whereas co-treatment with HGHL surprisingly increased *IL-6* expression compared to HGHL alone. This suggests that eugenol's regulation of *IL-6* may be context-dependent and influenced by the timing and nature of exposure.

Regarding *TNF-α*, the highest expression was observed in cells treated with HGHL alone. Co-treatment with E15 effectively reduced *TNF-α* expression, while post-treatment did not significantly lower *TNF-α* levels compared to HGHL/M. E15 treatment in untreated fibroblast cells showed a trend toward reduced baseline cytokine levels, suggesting potential anti-inflammatory properties.

Effect of HGHL and eugenol on the expression of ECM components

Proinflammatory cytokines such as IL-6 and TNF-α negatively impact ECM synthesis by downregulating the production of key structural proteins like collagen and elastin, which are essential for maintaining skin integrity and elasticity. Kuk (2014) demonstrated that TNF-α suppresses type I collagen expression in human dermal fibroblasts by inhibiting the transforming growth factor-beta (TGF-β)/Smad signaling pathway.[45] Similarly, Anwar et al. (2012) reported that IL-6 reduced elastin expression in vascular smooth muscle cells by modulating elastin gene promoter activity.[46] Although this finding pertains to smooth muscle cells, similar regulatory mechanisms are likely to occur in dermal fibroblasts.

The combined effects of elevated cytokine levels and diminished ECM protein expression can also hinder fibroblast migration, a key step in wound repair. Potekaev et al. (2021) emphasized the importance of ECM in supporting fibroblast motility[47], while Pastar et al. (2024) found that high TNF-α levels impaired fibroblast migration and proliferation by disrupting cytoskeletal organization and focal adhesion formation, ultimately delaying wound closure.[48]

Consistent with these findings, our study showed that HGHL conditions significantly reduced the expression of *COL1A1*, *COL3A1*, and *ELN* in fibroblasts. Additionally, wound healing assays revealed impaired fibroblast migration under these metabolic stress conditions. These results reinforce the idea that hyperglycemia and hyperlipidemia compromise ECM production and fibroblast function, thereby limiting tissue repair capacity.

Eugenol contributes to ECM preservation and skin regeneration through multiple mechanisms. It inhibits the formation of AGEs, which are detrimental sugar–protein or lipid complexes that stiffen the ECM, reduce elasticity, and accelerate skin aging. Eugenol lowers blood glucose levels and competes with sugars for binding to serum albumin, thereby protecting collagen integrity.[25] Furthermore, eugenols shield ECM components from both glycation and oxidative stress, supporting structural stability.[49] It also modulates pathways involved in ECM remodeling and cytokine–cytokine receptor interactions, which are crucial for tissue regeneration.[18]

The wound healing assay further confirmed eugenol's regenerative potential. Untreated fibroblasts exposed to 15 µM eugenol exhibited the fastest wound closure. While HGHL conditions impaired wound healing, both co-treatment and post-treatment with E15 slightly improved the rate of wound closure, although the effect was not statistically significant. These findings align with a study by Ashjazadeh et al. (2019), which demonstrated that eugenol-loaded nanofibers enhanced granulation tissue formation and collagen production in Wistar rats, thereby accelerating wound healing.[50] Their results support the hypothesis that eugenol promotes tissue regeneration by stimulating collagen synthesis and repair processes.

CONCLUSIONS AND FUTURE DIRECTIONS

In conclusion, this study provides compelling evidence that eugenol offers significant protective effects against skin aging and damage induced by HGHL conditions. Eugenol mitigates cellular senescence, apoptosis, oxidative stress, and inflammation through its antioxidant, anti-inflammatory, and AGE-reducing properties, while also promoting ECM synthesis and tissue regeneration. These findings support the potential of eugenol as a therapeutic agent for skin aging and tissue repair, offering a promising avenue for anti-aging skincare treatments. Further research is necessary to optimize the dosage and explore the long-term effects of eugenol in clinical settings.

Future research should focus on optimizing eugenol concentrations for different skin types and exploring its underlying molecular mechanisms, particularly related to oxidative stress, inflammation, and ECM remodeling. Long-term safety and efficacy need to be evaluated through animal models and clinical trials to assess its potential for topical skincare products. Investigating eugenol's synergy with other anti-aging compounds and its effects on various skin conditions, such as wound healing and inflammatory diseases, would expand its therapeutic applications. Additionally, exploring eugenol in advanced drug delivery systems could enhance its bioavailability and effectiveness in skin treatments.

Author Contributions: Conceptualization, F.N., E.G and I.K..; methodology, F.N., E.G., D.L, B.W., A.S., R.R.; validation, F.N., A.S., R.R.; formal analysis, F.N., A.S., E.G., B.W., D.L., R.R.; resources, I.K., O.K.; data curation, F.N., I.K.; writing—original draft preparation, F.N.; writing—review and editing, all; visualization, F.N., E.G., I.K.; supervision, I.K., O.K.; project administration, I.K., O.K.; funding acquisition, I.K., O.K. All authors have read and agreed to the published version of the manuscript.

Funding: This research was funded by MITACS, grant number IT28033.

Data Availability Statement: Available upon request.

Acknowledgments: N/a.

Conflicts of Interest: The authors declare no conflict of interest.

REFERENCES

1. Ouadi, S., Sierro, N., Goepfert, S., Bovet, L., Glauser, G., Vallat, A., ... & Ivanov, N. V. (2022). The clove (Syzygium aromaticum) genome provides insights into the eugenol biosynthesis pathway. Communications biology, 5(1): 684.
2. Hirose, S., Horiyama, S., Morikami, A., Fujiwara, K., & Tsukagoshi, H. (2024). Eugenol and Basil essential oil as priming agents for enhancing arabidopsis immune response. Bioscience, Biotechnology, and Biochemistry, zbae156.
3. Krasniqi, S., & Daci, A. (2017). Analgesics use in dentistry. Pharmacology, Toxicology and Pharmaceutical Science-Pain Relief-From Analgesics to Alternative Therapies, 24: 111-39.
4. Ulanowska, M., & Olas, B. (2021). Biological properties and prospects for the application of eugenol—a review. International journal of molecular sciences, 22(7): 3671.
5. Ghasemi Gojani, E., Rai, S., Norouzkhani, F., Shujat, S., Wang, B., Li, D., ... & Kovalchuk, I. (2024). Targeting β-cell plasticity: A promising approach for diabetes treatment. Current Issues in Molecular Biology, 46(7): 7621-7667.
6. Hussein, R. S., Bin Dayel, S., Abahussein, O., & El-Sherbiny, A. A. (2024). Influences on Skin and Intrinsic Aging: Biological, Environmental, and Therapeutic Insights. Journal of Cosmetic Dermatology, e16688.
7. Tong, T., Geng, R., Kang, S. G., Li, X., & Huang, K. (2024). Revitalizing Photoaging Skin through Eugenol in UVB-Exposed Hairless Mice: Mechanistic Insights from Integrated Multi-Omics. Antioxidants, 13(2): 168.
8. Shin, J. W., Kwon, S. H., Choi, J. Y., Na, J. I., Huh, C. H., Choi, H. R., & Park, K. C. (2019). Molecular mechanisms of dermal aging and antiaging approaches. International journal of molecular sciences, 20(9): 2126.
9. Rea, I. M., Gibson, D. S., McGilligan, V., McNerlan, S. E., Alexander, H. D., & Ross, O. A. (2018). Age and age-related diseases: role of inflammation triggers and cytokines. Frontiers in immunology, 9: 586.
10. Gkogkolou, P., & Böhm, M. (2012). Advanced glycation end products: key players in skin aging? Dermato-endocrinology, 4(3): 259-270.
11. Papaccio, F., Caputo, S., & Bellei, B. (2022). Focus on the contribution of oxidative stress in skin aging. Antioxidants, 11(6): 1121.
12. Chen, Y., Yu, C. Y., & Deng, W. M. (2019). The role of pro-inflammatory cytokines in lipid metabolism of metabolic diseases. International reviews of immunology, 38(6): 249-266.
13. Wang, Y., Xue, J., Li, Y., Zhou, X., Qiao, S., & Han, D. (2019). Telmisartan protects against high glucose/high lipid-induced apoptosis and insulin secretion by reducing the oxidative and ER stress. Cell biochemistry and function, 37(3): 161-168.
14. Sreedhar, A., Aguilera-Aguirre, L., & Singh, K. K. (2020). Mitochondria in skin health, aging, and disease. Cell death & disease, 11(6): 444.
15. Cong, J., Li, J. Y., & Zou, W. (2024). Mechanism and treatment of intracerebral hemorrhage focus on mitochondrial permeability transition pore. Frontiers in Molecular Neuroscience, 17: 1423132.
16. Almanza, A., Carlesso, A., Chintha, C., Creedican, S., Doultsinos, D., Leuzzi, B., ... & Samali, A. (2019). Endoplasmic reticulum stress signalling–from basic mechanisms to clinical applications. The FEBS journal, 286(2): 241-278.
17. Berlanga-Acosta, J. A., Guillén-Nieto, G. E., Rodríguez-Rodríguez, N., Mendoza-Mari, Y., Bringas-Vega, M. L., Berlanga-Saez, J. O., ... & Valdés-Sosa, P. A. (2020). Cellular senescence as the pathogenic hub of diabetes-related wound chronicity. Frontiers in Endocrinology, 11: 573032.
18. Damasceno, R. O. S., Pinheiro, J. L. S., Rodrigues, L. H. M., Gomes, R. C., Duarte, A. B. S., Emídio, J. J., ... & de Sousa, D. P. (2024). Anti-Inflammatory and Antioxidant Activities of Eugenol: An Update. Pharmaceuticals, 17(11): 1505.
19. Nisar, M. F., Khadim, M., Rafiq, M., Chen, J., Yang, Y., & Wan, C. C. (2021). Pharmacological properties and health benefits of eugenol: A comprehensive review. Oxidative medicine and cellular longevity, 2021(1): 2497354.
20. Sahlan, M., Tejamaya, M., Arbianti, R., Baruji, T., Adawiyah, R., & Hermansyah, H. (2021). The effects of nano-casein encapsulation and productions of a controlled-release on eugenol containing bio-pesticide toxicity. Key Engineering Materials, 874: 115-127.
21. Makuch, E., Nowak, A., Günther, A., Pełech, R., Kucharski, Ł., Duchnik, W., & Klimowicz, A. (2021). The effect of cream and gel vehicles on the percutaneous absorption and skin retention of a new eugenol derivative with antioxidant activity. Frontiers in Pharmacology, 12: 658381.
22. Bendre, R. S., Rajput, J. D., Bagul, S. D., & Karandikar, P. S. (2016). Outlooks on medicinal properties of eugenol and its synthetic derivatives. Nat Prod Chem Res, 4(3): 1-6.
23. Nagaraju, P. G., Sindhu, P., Dubey, T., Chinnathambi, S., CG, P. P., & Rao, P. J. (2021). Influence of sodium caseinate, maltodextrin, pectin and their Maillard conjugate on the stability, in vitro release, antioxidant activity. Food Hydrocolloids, 112: 106220.

24. Wanakhachornkrai, O., Banglao, W., Thongmee, A., & Sukplang, P. (2020). Determination of antioxidant, anti-aging and cytotoxicity activity of the essential oils from Cinnamomum zeylanicum. Journal of microbiology, biotechnology and food sciences, 10(3): 436-440.
25. Gojani, E. G., Wang, B., Li, D. P., Kovalchuk, O., & Kovalchuk, I. (2023). Anti-Inflammatory Properties of Eugenol in Lipopolysaccharide-Induced Macrophages and Its Role in Preventing β-Cell Dedifferentiation and Loss Induced by High Glucose-High Lipid Conditions. Molecules, 28(22): 7619.
26. Bian, X., Li, B., Yang, J., Ma, K., Sun, M., Zhang, C., & Fu, X. (2020). Regenerative and protective effects of dMSC-sEVs on high-glucose-induced senescent fibroblasts by suppressing RAGE pathway and activating Smad pathway. Stem cell research & therapy, 11: 1-16.
27. Chang, J., Li, Y., Huang, Y., Lam, K. S., Hoo, R. L., Wong, W. T., ... & Xu, A. (2010). Adiponectin prevents diabetic premature senescence of endothelial progenitor cells and promotes endothelial repair by suppressing the p38 MAP kinase/p16INK4A signaling pathway. Diabetes, 59(11): 2949-2959.
28. Zhang, Y., Xi, X., Mei, Y., Zhao, X., Zhou, L., Ma, M., ... & Yang, Y. (2019). High-glucose induces retinal pigment epithelium mitochondrial pathways of apoptosis and inhibits mitophagy by regulating ROS/PINK1/Parkin signal pathway. Biomedicine & Pharmacotherapy, 111: 1315-1325.
29. Römer, A., Linn, T., & Petry, S. F. (2021). Lipotoxic impairment of mitochondrial function in β-cells: A review. Antioxidants, 10(2): 293.
30. Oberhauser, L., & Maechler, P. (2021). Lipid-induced adaptations of the pancreatic beta-cell to glucotoxic conditions sustain insulin secretion. International Journal of Molecular Sciences, 23(1): 324.
31. Pole, A., Dimri, M., & Dimri, G. P. (2016). Oxidative stress, cellular senescence and ageing. AIMS molecular science, 3(3).
32. Song, S., Li, F., Zhao, B., Zhou, M., & Wang, X. (2024). Ultraviolet Light Causes Skin Cell Senescence: From Mechanism to Prevention Principle. Advanced Biology, 2400090.
33. Kim, D., Ahn, B. N., Kim, Y., Hur, D. Y., Yang, J. W., Park, G. B., ... & Lee, S. H. (2019). High glucose with insulin induces cell cycle progression and activation of oncogenic signaling of bladder epithelial cells cotreated with metformin and pioglitazone. Journal of Diabetes Research, 2019(1): 2376512.
34. Absalan, A., Mesbah-Namin, S. A., Tiraihi, T., & Taheri, T. (2017). Cinnamaldehyde and eugenol change the expression folds of AKT1 and DKC1 genes and decrease the telomere length of human adipose-derived stem cells (hASCs): An experimental and in silico study. Iranian Journal of Basic Medical Sciences, 20(3): 316.
35. Dodig, S., Čepelak, I., & Pavić, I. (2019). Hallmarks of senescence and aging. Biochemia medica, 29(3): 483-497.
36. Xu, R., Song, J., Ruze, R., Chen, Y., Yin, X., Wang, C., & Zhao, Y. (2023). SQLE promotes pancreatic cancer growth by attenuating ER stress and activating lipid rafts-regulated Src/PI3K/Akt signaling pathway. Cell Death & Disease, 14(8): 497.
37. Hamdulay, S. S., Wang, B., Birdsey, G. M., Ali, F., Dumont, O., Evans, P. C., ... & Mason, J. C. (2010). Celecoxib activates PI-3K/Akt and mitochondrial redox signaling to enhance heme oxygenase-1-mediumted anti-inflammatory activity in vascular endothelium. Free Radical Biology and Medicine, 48(8): 1013-1023.
38. Ghosh, R., Nadiminty, N., Fitzpatrick, J. E., Alworth, W. L., Slaga, T. J., & Kumar, A. P. (2005). Eugenol causes melanoma growth suppression through inhibition of E2F1 transcriptional activity. Journal of Biological Chemistry, 280(7): 5812-5819.
39. Zhuang, L., Jin, G., Hu, X., Yang, Q., Pei, X., & Zhao, W. (2022). TSPAN8 alleviates high glucose-induced apoptosis and autophagy via targeting mTORC2. Cell Biology International, 46(10): 1693-1703.
40. Wang, K., Chen, D., Yu, B., He, J., Mao, X., Huang, Z., ... & Luo, J. (2022). Eugenol alleviates transmissible gastroenteritis virus-induced intestinal epithelial injury by regulating NF-κB signaling pathway. Frontiers in immunology, 13: 921613.
41. Zhang, D., Jin, W., Wu, R., Li, J., Park, S. A., Tu, E., ... & Chen, W. (2019). High glucose intake exacerbates autoimmunity through reactive-oxygen-species-mediumted TGF-β cytokine activation. Immunity, 51(4): 671-681.
42. Du, G., Liu, C., Li, X., Chen, W., He, R., Wang, X., ... & Lan, W. (2016). Induction of matrix metalloproteinase-1 by tumor necrosis factor-α is mediumted by interleukin-6 in cultured fibroblasts of keratoconus. Experimental biology and medicine, 241(18): 2033-2041.
43. Shi, J., Fan, J., Su, Q., & Yang, Z. (2019). Cytokines and abnormal glucose and lipid metabolism. Frontiers in endocrinology, 10: 703.
44. Hasan, A., Akhter, N., Al-Roub, A., Thomas, R., Kochumon, S., Wilson, A., ... & Ahmad, R. (2019). TNF-α in combination with palmitate enhances IL-8 production via the MyD88-independent TLR4 signaling pathway: potential relevance to metabolic inflammation. International Journal of Molecular Sciences, 20(17): 4112.
45. Kuk, H. (2014). TAK1 Mediumtes TGF beta-1 Responses in Gingival Fibroblasts. The University of Western Ontario (Canada).
46. Anwar, M. A., Shalhoub, J., Lim, C. S., Gohel, M. S., & Davies, A. H. (2012). The effect of pressure-induced mechanical stretch on vascular wall

differential gene expression. Journal of vascular research, 49(6): 463-478.

47. Potekaev, N. N., Borzykh, O. B., Medvedev, G. V., Pushkin, D. V., Petrova, M. M., Petrov, A. V., ... & Shnayder, N. A. (2021). The role of extracellular matrix in skin wound healing. Journal of Clinical Medicine, 10(24): 5947.
48. Pastar, I., Balukoff, N. C., Sawaya, A. P., Vecin, N. M., & Tomic-Canic, M. (2024). Physiology and pathophysiology of wound healing in diabetes. In The Diabetic Foot: Medical and Surgical Management (pp. 109-134). Cham: Springer International Publishing.
49. Barboza, J. N., da Silva Maia Bezerra Filho, C., Silva, R. O., Medeiros, J. V. R., & de Sousa, D. P. (2018). An overview on the anti-inflammatory potential and antioxidant profile of eugenol. Oxidative medicine and cellular longevity, 2018(1): 3957262.
50. Ashjazadeh MA, Jahandideh A, Abedi G, Akbarzadeh A, Hesaraki S. Histopathology and Histomorphological Study of Wound Healing Using Clove Extract Nanofibers (Eugenol) Compared to Zinc Oxide Nanofibers on the Skin of Rats. Arch Razi Inst, 2019 Sep; 74(3): 267-277. doi:10.22092/ari.2018.120170.1184. Epub 2019 Oct 1. PMID: 31592592.